

# Deep learning method for lung cancer identification and classification

Sahil Jamdar<sup>1</sup>, Jayashree Vaddin<sup>1</sup>, Sachidanand B. Nargundkar<sup>1</sup>, Shrinivasa Patil<sup>2</sup>

<sup>1</sup>Department of Electronics Engineering, DKTE's TEI, Shivaji University, Maharashtra, India

<sup>2</sup>Department of Electronics and Telecommunication Engineering, DKTE's TEI, Shivaji University, Maharashtra, India

## Article Info

### Article history:

Received Sep 20, 2022

Revised Dec 7, 2023

Accepted Dec 20, 2023

### Keywords:

Convolution neural network

Deep learning

Detection and classification

Fully connected layer

Lung cancer

## ABSTRACT

Lung cancer (LC) is claiming many lives and is becoming a serious cause of concern. The detection of LC at an early stage assists the chances of recovery. Accuracy of detection of LC at an early stage can be improved with the help of a convolutional neural network (CNN) based deep learning approach. In this paper, we present two methodologies for Lung cancer detection (LCD) applied on Lung image database consortium (LIDC) and image database resource initiative (IDRI) data sets. Classification of these LC images is carried out using support vector machine (SVM), and deep CNN. The CNN is trained with i) multiple batches and ii) single batch for LC image classification as non cancer and cancer image. All these methods are being implemented in MATLAB. The accuracy of classification obtained by SVM is 65%, whereas deep CNN produced detection accuracy of 80% and 100% respectively for multiple and single batch training. The novelty of our experimentation is near 100% classification accuracy obtained by our deep CNN model when tested on 25 Lung computed tomography (CT) test images each of size 512×512 pixels in less than 20 iterations as compared to the research work carried out by other researchers using cropped LC nodule images.

*This is an open access article under the [CC BY-SA](https://creativecommons.org/licenses/by-sa/4.0/) license.*



## Corresponding Author:

Jayashree Vaddin

Department of Electronics Engineering, DKTE's TEI, Shivaji University

Maharashtra, India

Email: jayashreevaddin@gmail.com

## 1. INTRODUCTION

It is a fact that Lung cancer (LC) is the primary cause of carcinogenic death among men and women. Every year, numerous people die due to LC compared to that of breast, colon, and prostate cancers. As per American society of Lung cancer, newly identified lung cancer in recent year, makes around 1,918,030 new cases of lung cancer in the United States causing around 609,360 deaths [1]. In India, in a total of 5.26 million cancer cases, and 5.9% of cases are related to lung cancer [2]. Though LC is a serious disorder, some people are cured. In the India alone, 1.8 million people every year are identified with lung cancer. About 350,000, people identified with LC at some point are alive today due to early detection and treatment. So, early LC detection could be a boon for increasing the recovery chance of a patient.

Detection of LC based on few invasive techniques such as spiral computed tomography, sputum cytology, fluorescent bronchoscopy and lung cancer-related antigens are available but are limited in their findings w.r.to prior detection of LC [3]. Support vector machine (SVM) classifier is tested and found to be most suitable classifier for rice classification, data mining and skin disease detection [4]–[6]. Training the convolution neural network (CNN) for medical image classification is reported in [7]–[11]. Lung cancer detection by unsupervised pretraining on natural or medical images is reported in [12]–[15] followed by fine-

tuning on medical target images using CNN or other types of deep learning models. Barbu *et al.* [16] and Feulner *et al.* [17] explained there is report on analysis of three-dimensional patch creation for lung nodule detection and analysis on the extracted multi-level image features [18], [19].

Deep learning assisted with voting function for categorization of lung cancer presented by Rossetto *et al.* reported an accuracy of 97.5% with false positive rate less than 10% [20]. Sputum sample analysis manually needs a trained person to avoid errors besides it needs more time but results may be inaccurate [21]. Wu and Zhao reported Lung cancer detection (LCD) accuracy of 77.8% when tested on very small set of computed tomography (CT) lung images using supervised machine learning algorithm based on entropy degradation [22]. A review of various methods of LCD is reported by Kaur [23]. Taher and Sammouda presented two segmentation methods using neural network (NN) and a fuzzy c-mean (FCM) clustering algorithm, applied on colour sputum images to identify early stages of lung cancer [24]. Cervical cancer detection is studied by Intel group and have reported that, deep learning (DL) enhances accuracy by 81%," using intel technology [25].

Area quantification in hematoxylin and eosin stained samples with rich immune cells was analysed by Turkki *et al.* where deep CNN showed F-score of 0.94 [26]. The process was aided by an antibody-guided annotation. detection of lymph nodes (LN) in thoraco-abdominal region and classification of interstitial Lung disease (ILD) was studied by Shin *et al.* using transfer learning based CNN. Prediction of axial CT slices with ILD categories was reported by them achieving 85% sensitivity and false positive rate of 3%, on the mediastinal LN detection [27]. Krewer *et al.* researched on lung cancer detection [28] using Lung image database consortium (LIDC)-image database resource initiative (IDRI) (LIDC-IDRI) data set [29] and revealed that they could get classification accuracy of 90.9% for 33 CT images with specificity of 94.74%. For lung cancer detection, Rao *et al.* used a batch size of 20 during training the CNN keeping iterations as 1,000 and have reported a classification accuracy of 76% on LIDC-IDRI data set [30]. A LC image classification accuracy of 96% has been reported by Sasikala in [31] where they implemented CNN model on hundred, 20×20 pixels LC images. Abdul reported lung CT image classification accuracy of 97.2% where they worked on 28×28 nodule image size obtained from LIDC-IDRI [32]. Bhat *et al.* have shown that, CNN outperforms compared to the traditional methods in classifying the LIDC/IDRI lung CT images of size 40×40 pixels with an accuracy of 96.6% using three convolution blocks [33].

Deep learning techniques not only help to boost the accuracy of the early detection but also assist automation of the initial diagnosis of medical scans. So the purpose of this work is to design, implement and find an appropriate LC classification model that can differentiate between normal and cancerous lung CT images from LIDC-IDRI database [29]. Here we used CT images of size of 512×512 pixels instead of working on extracted nodule as reported in [31]–[33]. Our experimentation of arriving at the best model is based on the SVM and deep CNN classifiers. The statistical features obtained from preprocessed LC CT images are given as input to SVM classifier for classification into benign and malignant lung CT images. CNN based deep learning with single convolution block is used as a second method to classify lung CT images. Our experimentation using deep CNN model revealed 100% classification accuracy when tested on 25 test images of size 512×512 pixels.

## 2. THEORETICAL BACKGROUND

This section covers a brief preliminary about the two classifiers used in this paper viz.: SVM and deep CNN. SVM is the most sought-out tool for two class classification problems. CNN is immune to shift variance or space variance.

### 2.1. SVM

In two class classification data points are grouped into two independent classes by SVM. SVM computes the hyper-plane that isolates the two classes. This hyperplane is a line separating the plane into two fragments or classes in two-dimensional space. It uses a discriminative classifier to split the hyperplane where a singular data point is represented in n-dimensional space as a point with the estimation of each component being the prediction of a particular class. SVM algorithm finds an optimum hyperplane during training that categorizes new samples with label. Data points of SVM are features like correlation, homogeneity energy, entropy and contrast property as in (1)–(4) derived from gray level cooccurrence matrix (GLCM) of CT images. In all these  $P(i,j)$  is a cooccurrence value of a pair of pixel at coordinates  $(i,j)$ ,  $N$  is number of cooccurrence pairs,  $\mu$  is mean and sigma  $\sigma$  is standard deviation and  $\sigma^2$  variance.

- Correlation: It returns a metric for how closely a pixel is related to its neighbours throughout the entire image. A fully positively or negatively correlated image has a correlation of 1 or -1.

$$Correlation = \sum_{i,j=0}^{N-1} \frac{(i-\mu)(j-\mu)}{\sigma^2} \quad (1)$$

- Homogeneity: It returns a value that indicates closeness of GLCM's element to the diagonal elements of GLCM. For a diagonal GLCM, the range is [0 1], and is expressed as further.

$$Homoginiety = \sum_{i,j=0}^{N-1} \frac{P_{i,j}}{1+(1-j)^2} \quad (2)$$

- Energy: It is the GLCM's sum of squared elements. The location of the property energy is also termed as energy homogeneity or energy uniformity. Its range is between [0 1]. For a constant gray level, the energy is 1.

$$Energy = \sum_{i,j=0}^{N-1} (P_{i,j})^2 \quad (3)$$

- Entropy: This is a randomness metric that reaches its maximum value when all of elements are equal. The equation for entropy is as in (4).

$$Entropy = \sum_{i,j=0}^{N-1} -\ln(P_{i,j})P_{i,j} \quad (4)$$

- Contrast: It is the measures the local variations in the GLCM.

$$Contrast = \sum_{i,j=0}^{N-1} (i-j)P_{i,j} \quad (5)$$

## 2.2. CNN

Convolutional neural networks are known as artificial neural networks (ANN) with property of invariance to apace and shift depending upon their shared weights architecture and invariance characteristics. A CNN includes an input layer, output layer and multiple hidden layers. The hidden layers are usually made of convolutional layer, rectified linear unit (ReLU) layer, pooling layer, fully connected (FC) and normalization layers. The procedure of convolution is a cross-correlation rather than a convolution. The configuration of CNN depends upon the type and complexity of the issue to be solved with the projected output from the network. They are made up of two modules viz: the feature extractor and the classifier. The feature extractor is composed of convolutional and pooling layers followed by zero or more FC layers which form the classification module. This layer calculates the subsequent probabilities for the given input to fit in to one of the classes. Exclusion of the output layer along with the optional elimination of the last few fully connected layers transform the CNN from a classifier to a feature extractor.

## 2.3. CNN architecture for LCD

The architecture of CNN in LCD system consists of various layers such as image input layer, convolution layer, ReLu layer, max pooling, fully connected layer and softmax layer. as shown in Figure 1. The classification layer is configured to have two classes to classify lung CT images into non cancer and cancer classes. The input layer to this CNN has a lung CT image each of size 512×512 pixels. The LIDC-IDRI data set are used as input images to first input layer.

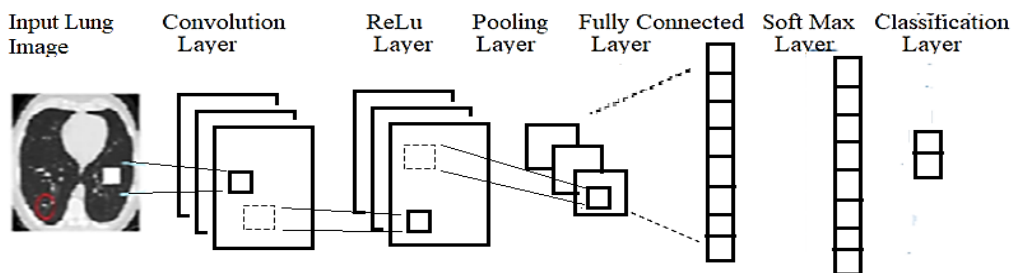


Figure 1. Layered architecture of CNN network

Convolution layer is the second layer for convolutional neural network (CNN). The input in 2-D convolutional layer is operated by sliding convolutional kernels moving horizontally and vertically along the

entire input image. The layer convolves the filter with input by calculating dot product of the weights and input, and includes bias term. Convolution operation of an image,  $I(a, b)$  with filter  $K(m, n)$  is represented as further.

$$s(t) = \sum_a \sum_b I(a, b) \cdot K(m - a, n - b) \quad (6)$$

Each convolutional 2D channel learns a different component in the input image and utilize them in a single layer to recognize various special features in each given image. These features may be edges and pixels with low intensities. When every filter is learnt out, then each of these filters are utilized as inputs to the rectified linear unit (ReLU) layer in the CNN. Here each input element is checked and set to zero if its value is less than zero. using a thresholding operation. Next layer in CNN is a Max pooling layer which helps to decrease the size of image by retaining maximum value in every  $2 \times 2$  nonoverlapping matrix of single slice. Thus, max pooling helps to retain the strongest activations and discards the other values.

Fully connected (FC) layer follows the pooling layer in CNN. Every neuron in the FC layer has a connection to every neuron in the preceding layer. It computes the probability score for classification into different classes. Thus, the high-level reasoning in the deep neural network (DNN) is accomplished via FC layers. In classification problems, the final FC layer is preceded by a softmax layer. The softmax function, normalizes taking  $K$  real input vectors into probabilities. Larger probabilities are assigned to large input components. Those network outputs without normalization are mapped into a probability distribution by softmax layer over a predicted output class. The last layer in deep CNN architecture is classification layer. It computes cross-entropy loss for multi-class classification problems. This layer takes input from the preceding output layer and assigns them to the predefined number of classes.

### 3. METHOD

Here the LC recognition system is realized using a neural network (NN) toolbox of MATLAB for implementation of SVM and CNN. Lung cancer imaging database, LIDC-IDRI [29] provided by the Cancer Imaging Archive public access community is used in this experimentation. This is a large dataset with over 1,200 patients having different cancer diseases in different parts of body. Only CT images with lung cancer are chosen as data set for our experimentation. The lung cancer images consisting of normal and abnormal status are chosen from LIDC-IDRI database. Figure 2 shows the lung CT sample images consisting of a) normal and b) Cancer CT image.

We have implemented two methodologies for Lung CT images classification a) SVM classifier and b) CNN based deep learning. Fourty five Lung CT images having width and height of  $512 \times 512$  pixels and with labels are obtained from LIDC database. Each patient dataset is labelled as positive or negative for cancer. The database has two groups viz: Lung cancer CT images for training, and for testing.

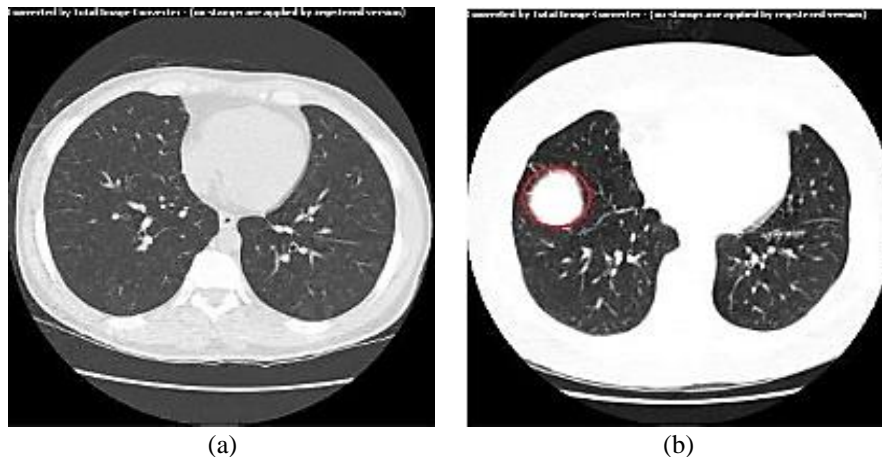


Figure 2. Lung CT scan images for, (a) Normal and (b) Cancer

The formulated and implemented block diagram for Lung cancer detection system (LCDS) is shown in the Figure 3. The input CT images are subjected to a pre-processing where they are converted from red green blue (RGB) image to grey and grey to black-white image and then given as input to both SVM and CNN. The

two approaches classify the lung CT images into Non cancer or the cancerous images. For classification using SVM, it takes the inputs that are features such as energy, contrast, correlation, and entropy that are extracted from cooccurrence matrix derived from preprocessed lung CT images of 512×512 pixels size.

In the deep CNN method, for the training and testing, preprocessed Lung CT images are presented to the input layer of CNN. CNN is trained using single batch and multiple batches using randomly selected images. For a single batch training, 20/10 CT images were used for training/testing respectively and an additional 15 images were kept aside to test the robustness of classification. Multiple batch training consisted of 3 batches with 20 CT scans in each batch. The output layer is designed to have two classes only, i.e., non cancer (benign), and cancer (malignant).

The architecture of the implemented CNN comprises of seven layers, as in Figure 1. During training of the CNN, the weights are randomly initialized and the parameters such as learning rate, maximum number of epochs, momentum of learning, number of filters/kernel and kernel size are used in the experimentation. The parameters of each layer of the designed CNN network are set before start of training to analyze the effect of parameters.

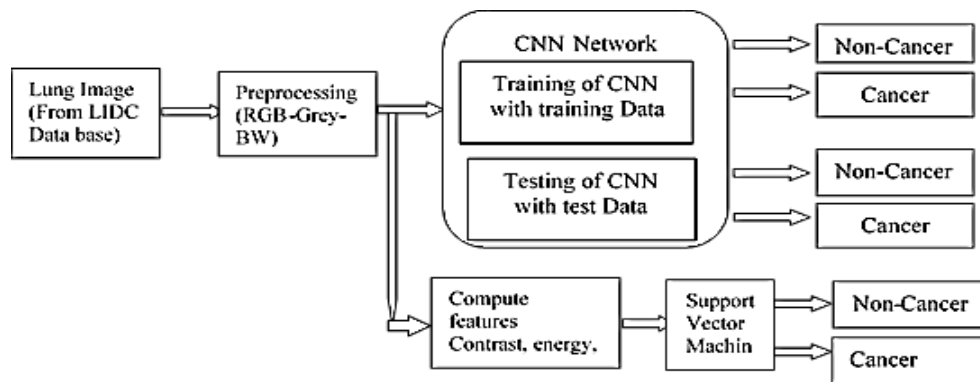


Figure 3. Shows the block diagram of the proposed LCDS

**4. RESULTS AND DISCUSSION**

Experimentation on LCD is carried out in three parts viz.: LCD using SVM, LCD using CNN with multiple batch training and LCD using CNN with single batch training. The result tables and quantitative analysis of these values are discussed further. These are detailed in subsections 4.1, 4.2, and subsection 4.3 respectively. Here we have used value '1'/'0' corresponding to Lung Cancer/normal Lung CT images.

**4.1. LCD using SVM**

Table 1. shows the accuracy of SVM for different input features selected. It is observed that the SVM classifier has produced an accuracy of 60% for each of the independent features like energy, correlation or, homogeneity considered one at a time and 65% for the contrast feature. Here wrongly classified LC image is indicated by bold letter in column of actual output. For e.g., the normal CT image classified as cancer image is indicated by bold letter 0. Since the accuracy obtained is low, deep CCN is implemented further and analyzed.

Table 1. Results of applying SVM for selected input features with 1-abnormal CT, 0-normal CT

Results of SVM with selected input features a) Energy, b) Correlation and c) Homogeneity (Kernel Function: linear)

No. of Images	Input Image	Input Feature	Actual Output 1 or 0	Desired Output 1 or 0	Accuracy	PR	PR	Time in Seconds
20	0,1,0,1,0,1,0,1,	Energy /Correlation/H omogeneity	1,0,1,0,0,0,0,	0,1,0,1,0,1,0,1,0	60 %	60 %	40 %	2.93
	0,1,0,1,0,1,0,		0,0,0,0,1,1,0,	,1, 0,1,0,1,0,				
	1,0,1,0,1		0,1,0,0,0,0	1,0,1,0,1				
20	0,1,0,1,0,1,0,1,	Contrast	0,0,0,0,0,0,0,	0,1,0,1,0,1,0,1,0	65 %	65 %	35 %	2.511
	0,1,0,1,0,1,0,		0,0,1,0,0,0,1,	,1,0,1,0,1,0,1,0,				
	1,0,1,0,1		0,0,0,1,0,0	1,0,1				

**4.2. LCD using deep CNN with multiple batch training**

For training a CNN with a large amount of database, multiple batch training gives the flexibility and improves the accuracy. Here the weights of the convolution layer are initialized randomly for the first batch,

and the next batch used the updated weights of previous batch for initialization. It is observed that, for batch 1, batch 2 and batch 3 training, the accuracy obtained is 70%/ 80% /80% respectively.

### 4.3. LCD using CNN with single batch training

The proposed CNN is trained using training set of 20 CT images which consisted of 10 normal lung CT images and 10 lung cancer CT images. The training images are alternate normal and abnormal lung CT images. The result analysis is divided into two parts: a) training results b) testing results as further.

#### 4.3.1. Training result analysis

For training total of 20 Lung CT scans were taken from LIDC dataset. Training is carried out by keeping CNN parameters kernel size, number of filters, pool size constant and the parameters viz.; a) momentum, b) initial learning rate, c) maximum epochs are varied one at a time. The CNN accuracy due to change in a) momentum, b) initial learning rate (LR), and c) kernel size is as shown in Tables 2 to 4 respectively. Observations from training Tables 2 and 3 reveal 100% CNN training accuracy for the momentum value of 0.9 in 57.01 secs and learning rate value of 0.01 in 68.41 secs.

Table 2. Accuracy result for varying momentum

Parameter values (const.): Initial Learning rate = 0.01, Max. epochs = 30, Kernel size = 5×5, No. of filters/kernels = 20.			
Sr. No.	Momentum	Accuracy	Time in Seconds
1	0.01	100 %	83.19
2	0.8	100 %	55.78
3	0.9	100 %	57.01

Table 3. Accuracy result for varying learning rate values

Parameter values (const.): Momentum = 0.9, Max. epochs = 30, Kernel size = 5×5, No. of filters/kernels = 20.			
Sr. No.	Initial Learning Rate	Accuracy	Time in seconds
1	0.001	100 %	68.93
2	0.01	100 %	68.41
3	0.1	50 %	61.50
4	0.2	50 %	57.29

Table 4 depicts the training experiment results carried out for finding optimum kernel size. Out of the experimented kernel sizes such as 3×3, 5×5 and 9×9, the kernel size of 3×3 produced 100% accurate training results in 39.96secs. Also, it is observed that, training with different epochs values of 5,10,20,30 have given 100% accuracy. However, a safe value of 30 epochs is chosen for further experimentation.

Table 4. Analysis of accuracy of training for different kernel sizes

Parameter values: Momentum = 0.9, Initial Learning rate = 0.01, Max. epochs = 30, No. of filters/kernels = 20, Stride = 2×2								
No. of images	Input Image	Kernel Size(s)	Actual Output (1 or 0)	Desired Output (1 or 0)	Accuracy	TPR	FPR	Time elapsed sec
20	0,1,0,1,0,1,0,1,0,1, 0,1,0,1,0,1,0,1,0,1	5×5 & 3×3	0,1,0,1,0,1,0, 1,0,1,0,1,0,1, 0,1,0,1,0,1	0,1,0,1,0,1,0,1,0, 1,0,1,0,1,0,1,0, 1,0,1	100 %	100 %	0%	40.175/39.96
20	1,0,1,0,1,0,1,0,1,0, 1,0,1,0,1,0,1,0,1,0	9×9	1,0,1,0,1,0,1, 0,1,0,1,0,1,0, 1,0,0,0,1,0	1,0,1,0,1,0,1,0,1, 0,1,0,1,0,1,0, 1,0,1,0	90 %	90%	10%	47.13

Observing the various training experimental results, the best performing training parameters found are convolution layer with 20 number of filters with filter size of 5×5, learning rate of 0.01 with 0.9 momentum, pool size 2 and stride of 2×2, max epochs of 30 and, fully connected layer with an output size of two classes as non cancerous and cancerous. These are used in experimentation further. Figure 4(a) and Figure 4(b) show the result graph of training accuracy vs. number of epochs and training loss vs. number of epochs respectively in Appendix. It took approximately 5/8 epochs respectively for achieving the results.

#### 4.3.2. Testing result analysis

Testing of lung CT images was carried out in two cycles with 10/15 lung CT image data respectively and by keeping the optimum CNN parameters. Accuracy of the detection of CNN network for test database is

shown in Table 5 which also depicts time of computation. Amongst the testing accuracy results obtained with variation in kernel size, the kernel size of 3×3 has given 100% testing accuracy in 0.944 seconds proving its efficacy. Performance of testing CNN network is evident in confusion matrix of Figure 5. Confusion matrix of Figure 5(a) for Test data set I and Figure 5(b) for Data set II respectively depict 100% accuracy of classification. Comparison of the different classification algorithms adopted is shown in Table 6. Here, it is found that SVM showed the least accuracy of 60% whereas CNN with single batch training produced higher accuracy than others. Comparison Table 7. reveals that our implemented CNN model performs better than the existing state-of-the-art of work by previous researchers.

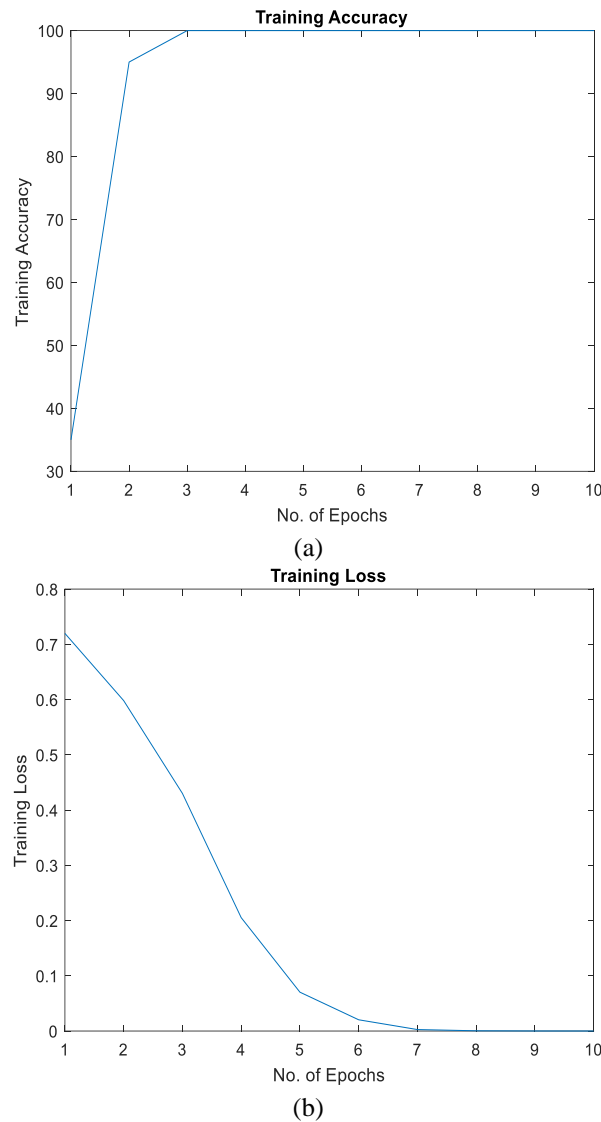


Figure 4. Plot of training (a) loss v/s number of epochs and (b) accuracy v/s number of epochs

Table 5. Testing accuracy of LCD with respect to the different kernel sizes

Set Parameter values: Momentum = 0.9, Initial Learning rate = 0.01, Max. epochs = 30, No. of filter = 20, Stride = 2×2									
Test Cycle	No. of Images	Input Test Image	Kernel Size(s)	Actual Output 1 or 0	Desired Output 1 or 0	Accuracy	TPR	FPR	Time seconds
I	10	1,0,0,0,1,	5×5 /3×3	1,0,0,0,1	1,0,0,0,1,	100%	100%	0%	1.999 /0.944
		1,1,0,1,0		,1,1,0,1,0	1,1,0,1,0				
II	15	1,1,1,1,1,	3×3	1,1,1,1,1,	1,1,1,1,1,	100%	100%	0%	1.5
		1,1,1,1,1,		1,1,1,1,1,	1,1,1,1,1,				
		1,1,1,1,1,		1,1,1,1,1,	1,1,1,1,1,				

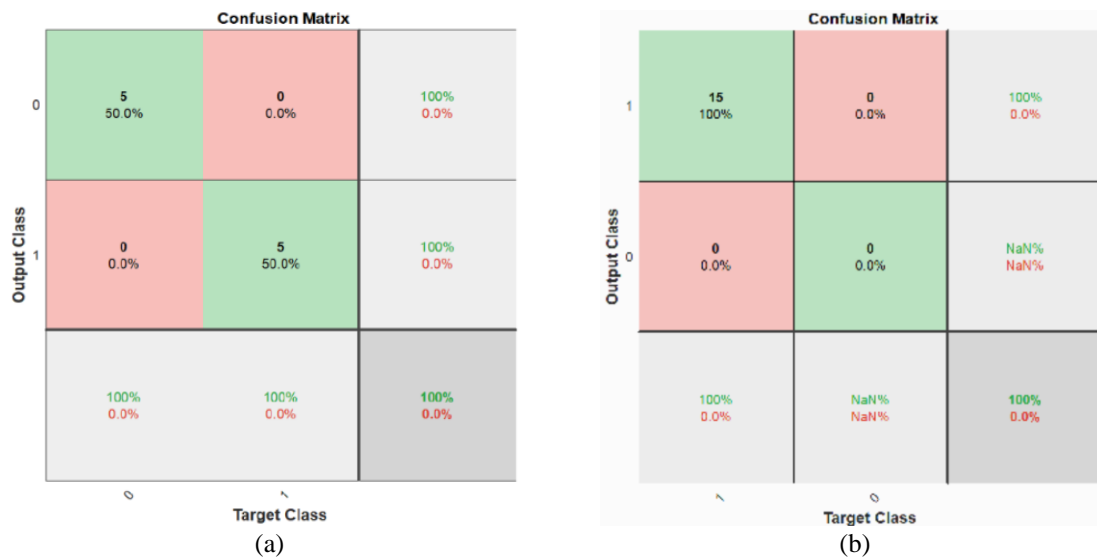


Figure 5. The confusion matrix result for testing with test data, (a) set I and (b) set II

Table 6. Comparison of different classification algorithms

Sr. No	Classifier	Input Feature/Batch training	Accuracy in %	TPR in %	FPR in %	Time elapsed in secs
1	SVM	Energy or Correlation or Homogeneity/--	60	60	40	2.93
2		Contrast	65	65	35	2.511
3	CNN	-/Batch-1	40	70	30	40.03
4		-/Batch-2	80	80	20	40.21
5		-/Batch-3	80	80	20	40.134
6	CNN	I-Single Batch	100	100	0	1.26
		II-Single Batch	100	100	0	2.5

Table 7. Comparison of proposed work with state-of art of research

Research Reference	Dataset /batch size/image size/learning rate/No. of Images/Conv layers	No. of Samples	Accuracy. (%)	Specificity. (%)	Sensitivity. (%)
[28]	LIDC-IDRI/-- /-	33	90.91	94.74	85.71
[30]	LIDC/ 20/128×128/0.001/71/2	71	76	-	-
[31]	LIDC/100/20×20 pixels/0.0001/3	100	96	1	0.875
[32]	LIDC/30/28×28/833/0.01/2	8296	97.2	95.6	96.1
[33]	LIDC-IDRI /100/888/40×40 /0.01/3	2948	96.6	FPR-0.018	ERR-0.034
Proposed Work	LIDC-IDRI /multi-20 & Single /512×512/0.01/ 25/1	45	100	0	TPR-100

## 5. CONCLUSION

We have presented CNN assisted deep learning method which classifies the 512×512-pixel size jpeg lung CT images into non cancer class or malignant class. For the analysis of lung CT scans, the color CT scans are pre-processed and converted to grey and then to black & white images. We used 20 CT scans for training data and 10(normal+abnormal)/15 abnormal CT scans for testing. We have reported two approaches, viz.; SVM classifier and CNN using multiple batch training and single5 batch training. The CNN approach with single batch training gave 100% accuracy of detection for lung cancer also has taken less time as compared to the other method justifying that our method is better than state of art of previous researchers works. So, we authentically conclude that the deep learning technique using CNN can be used to automate the early diagnosis of the lung cancer from the lung CT scans. Future\_scope would be to justify the robustness of the designed CNN by testing on a greater number of LC CT images and to measure the nodule size for classification of LC images as (i) unknown, (ii) benign, (iii) malignant, and (iv) metastatic state of cancer.

## ACKNOWLEDGEMENTS

Authors thank to the DKTE's Textile and Engineering Institute for the whole hearted support during the tenure of this dissertation work.






## REFERENCES

- [1] R. L. Siegel, K. D. Miller, H. E. Fuchs, and A. Jemal, "Cancer statistics, 2022," *CA: A Cancer Journal for Clinicians*, vol. 72, no. 1, pp. 7–33, 2022, doi: 10.3322/caac.21708.
- [2] N. Singh *et al.*, "Lung Cancer in India," *Journal of Thoracic Oncology*, vol. 16, no. 8, pp. 1250–1266, 2021, doi: 10.1016/j.jtho.2021.02.004.
- [3] F. M. Sullivan *et al.*, "Detection in blood of autoantibodies to tumour antigens as a case-finding method in lung cancer using the EarlyCDT®-Lung Test (ECLS): Study protocol for a randomized controlled trial," *BMC Cancer*, vol. 17, no. 1, 2017, doi: 10.1186/s12885-017-3175-y.
- [4] S. Ibrahim, N. Amirah Zulkifli, N. Sabri, A. Amilah Shari, and M. R. M. Noordin, "Rice grain classification using multi-class support vector machine (SVM)," *IAES International Journal of Artificial Intelligence (IJ-AI)*, vol. 8, no. 3, p. 215, Dec. 2019, doi: 10.11591/ijai.v8.i3.pp215-220.
- [5] A. Shmilovici, O. Maimon, and L. Rokach, "Data mining and knowledge discovery handbook," in *Springer*, O. Maimon and L. Rokach, Eds. Boston, MA: Springer US, 2009.
- [6] K. S. Parikh and T. P. Shah, "Support vector machine – a large margin classifier to diagnose skin illnesses," *Procedia Technology*, vol. 23, pp. 369–375, 2016, doi: 10.1016/j.protcy.2016.03.039.
- [7] B. H. Menze *et al.*, "The multimodal brain tumor image segmentation benchmark (BRATS)," *IEEE Transactions on Medical Imaging*, vol. 34, no. 10, pp. 1993–2024, 2015, doi: 10.1109/TMI.2014.2377694.
- [8] Y. Pan *et al.*, "Brain tumor grading based on Neural Networks and Convolutional Neural Networks," *Proceedings of the Annual International Conference of the IEEE Engineering in Medicine and Biology Society, EMBS*, vol. 2015-Novem, pp. 699–702, 2015, doi: 10.1109/EMBS.2015.7318458.
- [9] W. Shen, M. Zhou, F. Yang, C. Yang, and J. Tian, "Multi-scale convolutional neural networks for lung nodule classification," *Lecture Notes in Computer Science (including subseries Lecture Notes in Artificial Intelligence and Lecture Notes in Bioinformatics)*, vol. 9123, pp. 588–599, 2015, doi: 10.1007/978-3-319-19992-4\_46.
- [10] G. Carneiro, J. Nascimento, and A. P. Bradley, "Unregistered multiview mammogram analysis with pre-trained deep learning models," *Lecture Notes in Computer Science (including subseries Lecture Notes in Artificial Intelligence and Lecture Notes in Bioinformatics)*, vol. 9351, pp. 652–660, 2015, doi: 10.1007/978-3-319-24574-4\_78.
- [11] J. M. Wolterink, T. Leiner, B. D. de Vos, R. W. van Hamersvelt, M. A. Viergever, and I. Išgum, "Automatic coronary artery calcium scoring in cardiac CT angiography using paired convolutional neural networks," *Medical Image Analysis*, vol. 34, pp. 123–136, 2016, doi: 10.1016/j.media.2016.04.004.
- [12] T. Schlegl, J. Ofner, and G. Langs, "Unsupervised pre-training across image domains improves lung tissue classification," *Lecture Notes in Computer Science (including subseries Lecture Notes in Artificial Intelligence and Lecture Notes in Bioinformatics)*, vol. 8848, pp. 82–93, 2014, doi: 10.1007/978-3-319-13972-2\_8.
- [13] J. Hofmanninger and G. Langs, "Mapping visual features to semantic profiles for retrieval in medical imaging," *Proceedings of the IEEE Computer Society Conference on Computer Vision and Pattern Recognition*, vol. 07-12-June, pp. 457–465, 2015, doi: 10.1109/CVPR.2015.7298643.
- [14] G. Carneiro and J. C. Nascimento, "Combining multiple dynamic models and deep learning architectures for tracking the left ventricle endocardium in ultrasound data," *IEEE Transactions on Pattern Analysis and Machine Intelligence*, vol. 35, no. 11, pp. 2592–2607, 2013, doi: 10.1109/TPAMI.2013.96.
- [15] R. Li *et al.*, "Deep learning based imaging data completion for improved brain disease diagnosis," *Lecture Notes in Computer Science (including subseries Lecture Notes in Artificial Intelligence and Lecture Notes in Bioinformatics)*, vol. 8675 LNCS, no. PART 3, pp. 305–312, 2014, doi: 10.1007/978-3-319-10443-0\_39.
- [16] A. Barbu, M. Suehling, Xun Xu, D. Liu, S. K. Zhou, and D. Comaniciu, "Automatic Detection and Segmentation of Lymph Nodes From CT Data," *IEEE Transactions on Medical Imaging*, vol. 31, no. 2, pp. 240–250, Feb. 2012, doi: 10.1109/TMI.2011.2168234.
- [17] J. Feulner, S. Kevin Zhou, M. Hammon, J. Horneegger, and D. Comaniciu, "Lymph node detection and segmentation in chest CT data using discriminative learning and a spatial prior," *Medical Image Analysis*, vol. 17, no. 2, pp. 254–270, 2013, doi: 10.1016/j.media.2012.11.001.
- [18] L. Lu, P. Devarakota, S. Vikal, D. Wu, Y. Zheng, and M. Wolf, "Computer aided diagnosis using multilevel image features on large-scale evaluation," *Lecture Notes in Computer Science (including subseries Lecture Notes in Artificial Intelligence and Lecture Notes in Bioinformatics)*, vol. 8331 LNCS, pp. 161–174, 2014, doi: 10.1007/978-3-319-05530-5\_16.
- [19] L. Lu, J. Bi, M. Wolf, and M. Salganicoff, "Effective 3D object detection and regression using probabilistic segmentation features in CT images," *Proceedings of the IEEE Computer Society Conference on Computer Vision and Pattern Recognition*, pp. 1049–1056, 2011, doi: 10.1109/CVPR.2011.5995359.
- [20] A. M. Rossetto and W. Zhou, "Deep learning for categorization of lung cancer CT images," *Proceedings - 2017 IEEE 2nd International Conference on Connected Health: Applications, Systems and Engineering Technologies, CHASE 2017*, pp. 272–273, 2017, doi: 10.1109/CHASE.2017.98.
- [21] H. Yang, H. Yu, and G. Wang, "Deep learning for the classification of lung nodules," 2016.
- [22] Q. Wu and W. Zhao, "Small-cell lung cancer detection using a supervised machine learning algorithm," *Proceedings - 2017 International Symposium on Computer Science and Intelligent Controls, ISCSIC 2017*, vol. 2018-Febru, pp. 88–91, 2018, doi: 10.1109/ISCSIC.2017.22.
- [23] S. Kaur, "Comparative study review on lung cancer detection using neural network and clustering algorithm," *IJARECE Journal*, vol. 4, no. 2, pp. 169–174, 2015.
- [24] F. Taher and R. Sannouda, "Artificial neural network and fuzzy clustering methods in segmenting sputum color images for lung cancer diagnosis." In *Image and Signal Processing: 4th International Conference, ICISP 2010, Trois-Rivières, QC, Canada, June 30-July 2, 2010. Proceedings 4*, pp. 513-520. 2010.
- [25] I. on Kaggle and M. Competition, "Deep learning improves cervical cancer accuracy by 81%, using intel technology," *December 22, 2017*.
- [26] R. Turkki, N. Linder, P. E. Kovanen, T. Pellinen, and J. Lundin, "Antibody-supervised deep learning for quantification of tumor-infiltrating immune cells in hematoxylin and eosin stained breast cancer samples," *Journal of Pathology Informatics*, vol. 7, no. 1, 2016, doi: 10.4103/2153-3539.189703.
- [27] H. C. Shin *et al.*, "Deep convolutional neural networks for computer-aided detection: CNN architectures, dataset characteristics and transfer learning," *IEEE Transactions on Medical Imaging*, vol. 35, no. 5, pp. 1285–1298, 2016, doi: 10.1109/TMI.2016.2528162.
- [28] H. Krewer *et al.*, "Effect of texture features in computer aided diagnosis of pulmonary nodules in low-dose computed tomography," *Proceedings - 2013 IEEE International Conference on Systems, Man, and Cybernetics, SMC 2013*, pp. 3887–3891, 2013, doi: 10.1109/SMC.2013.663.




- [29] National Cancer Institute, "Cancer imaging archive," *National Institutes of Health*, 2022.
- [30] P. Rao, N. A. Ferreira, and R. Srinivasan, "Convolutional neural networks for lung cancer screening in computed tomography (CT) scans," *Proceedings of the 2016 2nd International Conference on Contemporary Computing and Informatics, IC3I 2016*, pp. 489–493, 2016, doi: 10.1109/IC3I.2016.7918014.
- [31] S. Sasikala, M. Bharathi, and B. R. Sowmiya, "Lung cancer detection and classification using deep learning," *International Journal of Innovative Technology and Exploring Engineering (IJITEE)*, vol. 8, no. 2S, pp. 259–262, 2018, doi: 10.1109/ICCUBEA.2018.8697352.
- [32] W. Abdul, "An automatic lung cancer detection and classification (ALCDC) system using convolutional neural network," in *2020 13th International Conference on Developments in eSystems Engineering (DeSE)*, Dec. 2020, pp. 443–446, doi: 10.1109/DeSE51703.2020.9450778.
- [33] S. Bhat, R. Shashikala, S. Kumar, and K. Gururaj, "Convolutional neural network approach for the classification and recognition of lung nodules," *Proceedings of the 4th International Conference on Electronics, Communication and Aerospace Technology, ICECA 2020*, pp. 1310–1314, 2020, doi: 10.1109/ICECA49313.2020.9297626.

## BIOGRAPHIES OF AUTHORS






**Sahil Jamdar**    is a M. Tech Electronics student at DKTE's Textile and Engineering Institute during which period he carried out, a dissertation work on lung cancer detection. He is a very sincere, intelligent and hard-working student & secured gold medal in M.Tech. He is currently serving in TCS. His research interests include Computer Vision and AI, and VLSI Design. He can be contacted at email: sahilj2244@gmail.com.






**Dr. Jayashree Vaddin, Ph.D.**    (Electronics, 2013), received M.E. (Electronics, 1997) from Shivaji University, India, & B.E. (Electrical, 1983), Karnatak University. She served as a Professor PG Electronics, and HOD Electrical Engineering & has set up VLSI design lab using Cadence Tool under AICTE grant. Her research fields are Image processing & AI, VLSI Design and Automation. She has published 70 research papers, 4 technical books, & filed one patent, and has delivered 18 expert lectures. 20 students have completed PG under her & is guiding 6 PhD students She has won many awards and is a Senior member IEEE, since 2019. She can be contacted at email: jayashreevaddin@gmail.com.



**Sachidanand B. Nargundkar**    is a Faculty of M.Tech. Electronics at DKTE's TEI holds a UG in Electronics & communication Engineering, PG degree in Digital Electronics from B.V.B College of Engineering, Karnataka. He is teaching for PG and UG & has 9 years of teaching experience. His research interests are Digital systems, Signal and systems, data structures and VLSI design. He has published 6 papers in journals and has coordinated various workshops. He can be contacted at email: sachidanandbn@gmail.com.



**Dr. Shrinivas Patil**    a Professor and H.O.D. of ETC at DKTE's TEI, obtained B.E./Ph.D. degrees in 1988/2011 resp. both from Shivaji University, Kolhapur in Electronics Engineering preceded by PG in Bio-Medical Engg., I.I.T. Bombay in 1997. His research areas include Medical Electronics, Embedded Systems, and VLSI Systems designing. He has completed 18 consultancy projects, 6 technical books, 63 publications, and 12 review articles, & filed six patents. Currently has 10 PG / 8 Ph.D. students, & one student completed Ph.D. under him and has won many awards. He can be contacted at email: shrinivasapatil@gmail.com.